Pergamon

Int. J. Solids Structures Vol. 35, No. 12, pp. 1199–1217, 1998

0020–7683/98 $19.00 + .00

PII: S0020–7683(97)00099–1

VIBRATION OF POSTBUCKLED DELAMINATED BEAM-PLATES

T.-P. CHANG and J.-Y. LIANG
Department of Applied Mathematics, National Chung-Hsing University, Taichung, Taiwan 40227, Republic of China

(*Received* 2 *June* 1996; *in revised form* 26 *March* 1997)

Abstract—In this study, the free and forced vibrations of postbuckled delaminated beam-plates have been investigated. If a beam-plate is under a postbuckled state, the natural frequencies, mode shapes of the structure will be substantially affected by the changes of the size and location of the delamination and by the magnitude of the axial compression. Based on the revised boundary conditions and governing partial differential equations, the natural frequencies and mode shapes of the postbuckled delaminated beam-plates are calculated by using the separation of variables. Once the natural frequencies and mode shapes are accomplished, the dynamic responses of the postbuckled delaminated beam-plate can be obtained readily. © 1998 Elsevier Science Ltd.

1. INTRODUCTION

The applications of composite materials, due to their strength and specific stiffness, have been increasing broadly in the fields of aircraft, ships and etc. However, the strength and the rigidity of the composite laminate will be affected significantly by the geometrical and material defects, which may occur in the imperfect manufacturing process or it may be produced by the external loads during the operational life. Recently, the study of delamination buckling in composite laminates has been very important and prospering. These problems can be solved in both analytical methods and numerical methods such as the finite element method.

The free vibrations of split beams were researched by Wang *et al.* (1982). They observed that the fundamental frequency was not visibly reduced due to the short delamination and was in agreement with the experimental results. Later, numerous papers discussed the postbuckling problems, which are described as follows. Simitses *et al.* (1985) studied the buckling load of the delaminated homogeneous laminated plates with arbitrary delaminated location. The results indicated that the buckling load could serve as a measure of the load-carrying capacity of the delaminated configuration for certain geometry. Yin *et al.* (1986) also found that the postbuckling axial load could be considerably greater than the buckling load, while the failure of the plate might or might not be governed by the delamination growth. Moreover, the deformation of delaminated composites under axial compression was investigated in a one-dimensional (1-D) beam-plate model by Kardomateas and Schmueser (1988). In this model, analytical solutions for the critical instability load and postbuckling deflections were obtained by using the perturbation technique. At the same time, Yin and Fei (1988) presented an elastic postbuckling analysis of a delaminated circular plate under axisymmetric compression along its clamped boundary, and discovered that certain features of the postbuckling behavior of the delaminated circular plate were similar to those of a delaminated beam-plate subjected to an axial load. Later, based on the large deflection of the delaminated layer, the postbuckling deformation of composites with thin delamination was modeled by Kardomateas (1989). The results of this paper could be expressed as a sequence of the transverse deflections which would not be limited to the postbuckled shape of the beam, a reduced stiffness was predicted and the end fixity conditions violently affected the postbuckling behavior. Besides, the experiments were also performed and discussed with thin delaminations.

With the transverse shear effect, the buckling and delamination growth for various length ratios and thickness ratios of the delaminated beam-plate were calculated by Chen

(1991) and compared with those without the shear effect. Shen and Grady (1992) evaluated the free vibrations of delaminated beams by analytical and experimental methods, the calculated natural frequencies and mode shapes of the delaminated beam were hugely affected by the coupling effect of the axial loads and bending moments. Furthermore, refer to the postbuckled states, the free vibrations of the beam-plate with a symmetric delamination respecting to the mid-point were investigated using the perturbation technique by Yin and Jane (1992), the small amplitude vibration relative to a static postbuckled state were considered in this paper. Lately, the finite element analysis was adopted to study the delamination problems. Davila and Johnson (1993) used a finite element method to calculate the compression strength of the postbuckled delaminated dropped-ply laminates and verified the results by experiments. Finally, the free vibration of the beam-plate, having an arbitrary delamination with respect to a postbuckled state, was investigated using the perturbation technique by Jane and Chen (1995) and the postbuckling deformation was also calculated.

In the present work, we study the free and forced vibrations of the postbuckled delaminated beam-plate subjected to an axial load and with two clamped edges. We deal with a homogeneous isotropic beam-plate containing an arbitrary across-the-width delamination. The original boundary conditions of the problem are not homogeneous so that the revised procedure must be adopted to accomplish the homogeneous boundary conditions, then the separation of variables can be used to get the natural frequencies and mode shapes of the free vibration problem, furthermore, the forced vibration analysis can be performed.

2. FORMULATION OF THE PROBLEM

In the present analysis, the configuration under study is represented in the sketch of Fig. 1 and consists of a homogeneous, isotropic beam-plate of thickness h and of unit width containing an arbitrary, parallel delamination at depth h_3 from the top surface of the beam-plate, although the present analysis may be extended to strip delamination models with a general laminate structure. The beam-plate is clamped and compressed by the axial load p at the two edges in the initial state. The length of the single delamination is a and the left tip of the delamination is located at length l_1 from the left edge of the beam-plate.

We investigate the vibration relative to the static postbuckling state, and the delaminated beam-plate is divided into four segments, the governing equations of these segments are as follows:

$$D_i\frac{\partial^4 w_i}{\partial x^4}+p_i\frac{\partial^2 w_i}{\partial x^2}+m_i\frac{\partial^2 w_i}{\partial t^2}=f(x,t),\quad i=1,2,3 \tag{1}$$

$$D_i\frac{\partial^4 w_i}{\partial x^4}+p_i\frac{\partial^2 w_i}{\partial x^2}+m_i\frac{\partial^2 w_i}{\partial t^2}=0,\quad i=4 \tag{2}$$

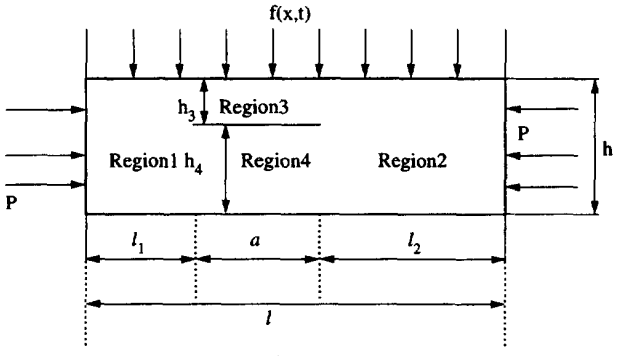

Fig. 1. One-dimensional delamination model.

where the bending stiffness D_i depending on the thickness h_i of the ith segment, Young's modulus E and Poisson ratio v is equal to $Eh_i^3/[12(1-v^2)]$, $f(x,t)$ is the external force, p_i is the axial load of the ith segment and m_i is the mass per unit length of ith segment. In eqns (1) and (2), $p_1 = p_2 = p$ and $p_3 + p_4 = p$, where p is greater than the buckling load of the delaminated beam-plate, according to a previous analysis done by Simitses *et al.* (1985). p_3, p_4 and the static deformation $w_i^{(s)}(x)$ done by Jane and Chen (1995) can be determined by the clamped boundary conditions, the continuity of deflection at both delaminated tips, the continuity of rotation at both delaminated tips, the balance of the bending moments and shear forces at the both tips, and the compatibility of axial shortening.

Once we impose the initial and boundary conditions on the governing equations, we should be able to obtain the solution of the vibration relative to the postbuckling state. The coordinate systems have been selected to satisfy the boundary conditions in such a way that the deflections and the slopes of deflections are zero at the two edges of the beam-plate, therefore, the clamped boundary conditions can be written as

$$w_1(0,t) = 0 \tag{3a}$$

$$w_1'(0,t) = 0 \tag{3b}$$

$$w_2(l_2,t) = 0 \tag{3c}$$

$$w_2'(l_2,t) = 0. \tag{3d}$$

The one-dimensional (1-D) model is assumed to be continuous, these different segments have common positions at both delaminated tips, so the continuity of deflection at the two positions must be satisfied and can be written as

$$w_1(l_1,t) = w_3(0,t) \tag{3e}$$

$$w_3(0,t) = w_4(0,t) \tag{3f}$$

$$w_3(a,t) = w_4(a,t) \tag{3g}$$

$$w_2(0,t) = w_3(a,t). \tag{3h}$$

The continuity of rotation is that the slopes of the deflection are all the same for the 1st, 3rd and 4th segments at both delaminated tips, similar for the 2nd, 3rd and 4th segments and can be written as follows

$$w_1'(l_1,t) = w_3'(0,t) \tag{3i}$$

$$w_3'(0,t) = w_4'(0,t) \tag{3j}$$

$$w_3'(a,t) = w_4'(a,t) \tag{3k}$$

$$w_2'(0,t) = w_3'(a,t). \tag{3l}$$

The corresponding moments and shear forces for these different segments are denoted by M_i, V_i. Furthermore, the balance of bending moments and shear forces at both tips of the delamination can be written as

$$-M_1(l_1,t) + M_3(0,t) + M_4(0,t) - \frac{p_4 h_3}{2} + \frac{p_3 h_4}{2} = 0 \tag{3m}$$

$$M_2(0,t) - M_3(a,t) - M_4(a,t) - \frac{p_3 h_4}{2} + \frac{p_4 h_3}{2} = 0 \tag{3n}$$

$$V_1(l_1,t) - V_3(0,t) - V_4(0,t) = 0 \tag{3o}$$

$$V_2(0,t) - V_3(a,t) - V_4(a,t) = 0. \tag{3p}$$

The initial conditions are only the initial static postbuckling deflections which are related to the axial compressive load p, the length of the delamination a, the length of the beam-plate l, the thickness of the beam-plate h and the location of the delamination. The axial load is greater than the buckling load of the delaminated beam-plate and only the upper part has apparent significant deformation, then the crack is explicitly open, and the initial conditions can be written as follows:

$$w_i(x,0) = w_i^{(s)}(x) \quad \text{for } i = 1,2,3,4. \tag{4}$$

It should be noted that among all the boundary conditions, eqns (3m) and (3n) are not homogeneous. In order to adopt separation of variables, the boundary conditions must be revised to become homogeneous form which can be done by the following transformation, which has been discussed and adopted by Meirovitch (1967). Let

$$w_i(x,t) = u_i(x,t) + a_i x^3 + b_i x^2 + c_i x + d_i, \quad i = 1,2,3,4. \tag{5}$$

Then, the revised boundary conditions of revised deformation $u_i(x,t)$ are homogeneous and a_i, b_i, c_i, d_i can be determined from eqns (3a)–(3p). Substituting eqn (5) into eqns (3a)–(3p), we can obtain the following equations:

$$d_1 = 0 \tag{6a}$$

$$c_1 = 0 \tag{6b}$$

$$a_2 l_2^3 + b_2 l_2^2 + c_2 l_2 + d_2 = 0 \tag{6c}$$

$$3a_2 l_2^2 + 2b_2 l_2 + c_2 = 0 \tag{6d}$$

$$a_1 l_1^3 + b_1 l_1^2 + c_1 l_1 + d_1 = d_3 \tag{6e}$$

$$d_3 = d_4 \tag{6f}$$

$$a_3 a^3 + b_3 a^2 + c_3 a + d_3 = a_4 a^3 + b_4 a^2 + c_4 a + d_4 \tag{6g}$$

$$d_2 = a_3 a^3 + b_3 a^2 + c_3 a + d_3 \tag{6h}$$

$$3a_1 l_1^2 + 2b_1 l_1 + c_1 = c_3 \tag{6i}$$

$$c_3 = c_4 \tag{6j}$$

$$3a_3 a^2 + 2b_3 a + c_3 = 3a_4 a^2 + 2b_4 a + c_4 \tag{6k}$$

$$c_2 = 3a_3 a^2 + 2b_3 a + c_3 \tag{6l}$$

$$-D_1(6a_1 l_1 + 2b_1) + D_3(2b_3) + D_4(2b_4) - \frac{p_4 h_3}{2} + \frac{p_3 h_4}{2} = 0 \tag{6m}$$

$$-D_2(2b_2) + D_3(6a_3 a + 2b_3) + D_4(6a_4 a + 2b_4) - \frac{p_4 h_3}{2} + \frac{p_3 h_4}{2} = 0 \tag{6n}$$

$$D_1(6a_1) - D_3(6a_3) - D_4(6a_4) = 0 \tag{6o}$$

$$D_2(6a_2) - D_3(6a_3) - D_4(6a_4) = 0. \tag{6p}$$

Equations (6a)–(6p) provide 16 linear equations for 16 variables a_i, b_i, c_i, d_i, $i = 1, 2, 3, 4$, and yield a linear, algebraic and nonhomogeneous system which expressed the equation below. Consequently, we can obtain the nontrivial solution for the unknowns a_i, b_i, c_i and d_i, that is

$$[M]\{X\} = \{b\} \tag{7}$$

where

$$\{X\} = [a_1, b_1, c_1, d_1, a_2, b_2, c_2, d_2, a_3, b_3, c_3, d_3, a_4, b_4, c_4, d_4]^T$$

$$\{b\} = \left[0, 0, 0, 0, 0, 0, 0, 0, 0, 0, 0, 0, \frac{p_4 h_3 - p_3 h_4}{2}, \frac{p_3 h_4 - p_4 h_3}{2}, 0, 0\right]^T.$$

The elements of M are related to the length of the intact regions, the length of the delaminated region and the ith bending stiffness of the ith region.

Following the previous procedure, we have already revised the nonhomogeneous boundary conditions. Therefore, we can establish the revised governing equations, the revised boundary conditions which are homogeneous and the revised initial conditions. The revised governing equations can be obtained by substituting eqn (5) into eqns (1) and (2), we find that the revised term of the external transverse force for the four regions are related to the axial load of the ith region, the coefficients of the eqn (5) and the external transverse force itself. Because the revised boundary conditions are homogeneous, now we can solve the revised deformation $u_i(x, t)$ by separation of variables. The expressions of the revised governing equations are

$$D_i \frac{\partial^4 u_i}{\partial x^4} + p_i \frac{\partial^2 u_i}{\partial x^2} + m_i \frac{\partial^2 u_i}{\partial t^2} = f(x, t) - 6p_i a_i x - 2p_i b_i, \quad i, = 1, 2, 3 \tag{8}$$

$$D_i \frac{\partial^4 u_i}{\partial x^4} + p_i \frac{\partial^2 u_i}{\partial x^2} + m_i \frac{\partial^2 u_i}{\partial t^2} = -6p_i a_i x - 2p_i b_i, \quad i = 4. \tag{9}$$

The revised boundary conditions consist of the clamped boundary conditions, the continuity of deflection and rotation at both delaminated tips and the balance of the bending moments and the shear forces at both tips. The boundary conditions of eqns (8) and (9) have been made to be homogeneous by the revised procedure and are given as follows:

$$u_1(0, t) = 0 \tag{10a}$$

$$u_1'(0, t) = 0 \tag{10b}$$

$$u_2(l_2, t) = 0 \tag{10c}$$

$$u_2'(l_2, t) = 0 \tag{10d}$$

$$u_1(l_1, t) = u_3(0, t) \tag{10e}$$

$$u_3(0, t) = u_4(0, t) \tag{10f}$$

$$u_3(a, t) = u_4(a, t) \tag{10g}$$

$$u_2(0, t) = u_3(a, t) \tag{10h}$$

$$u_1'(l_1, t) = u_3'(0, t) \tag{10i}$$

$$u_3'(0, t) = u_4'(0, t) \tag{10j}$$

$$u_3'(a, t) = u_4'(a, t) \tag{10k}$$

$$u_2'(0, t) = u_3'(a, t) \tag{10l}$$

$$-M_1(l_1, t) + M_3(0, t) + M_4(0, t) = 0 \tag{10m}$$

$$M_2(0, t) - M_3(a, t) - M_4(a, t) = 0 \tag{10n}$$

$$V_1(l_1, t) - V_3(0, t) - V_4(0, t) = 0 \tag{10o}$$

$$V_2(0, t) - V_3(a, t) - V_4(a, t) = 0. \tag{10p}$$

The original initial conditions for $w_i(x,t)$ are assumed that only the initial static deformations $w_i^{(s)}(x)$, based on the revised procedure, the revised initial conditions of the delaminated beam-plate which consist of the initial static deformation and the polynomial of eqn (5) can be obtained by substituting eqn (5) into eqn (4) as follows:

$$u_1(x,0) = w_1^{(s)}(x) - a_1x^3 - b_1x^2 - c_1x - d_1 \tag{11a}$$

$$u_2(x,0) = w_2^{(s)}(x) - a_2x^3 - b_2x^2 - c_2x - d_2 \tag{11b}$$

$$u_3(x,0) = w_3^{(s)}(x) - a_3x^3 - b_3x^2 - c_3x - d_3 \tag{11c}$$

$$u_4(x,0) = w_4^{(s)}(x) - a_4x^3 - b_4x^2 - c_4x - d_4. \tag{11d}$$

3. FREE VIBRATION ANALYSIS

Once we have accomplished the revised system including the revised nonhomogeneous governing equations, the revised homogeneous boundary conditions and the revised initial conditions, we should be able to calculate the revised deformation by separation of variables, that is, assuming $u_i(x,t) = Y_i(x)T_i(t)$. In order to perform the free vibration analysis, we solve the generalized displacement $Y_i(x)$ from the corresponding homogeneous P.D.E. of eqns (8) and (9) as follows:

$$D_i\frac{\partial^4 u_i}{\partial x^4} + p_i\frac{\partial^2 u_i}{\partial x^2} + m_i\frac{\partial^2 u_i}{\partial t^2} = 0, \quad i = 1,2,3,4 \tag{12}$$

$$\frac{D_iY_i'''' + p_iY_i''}{m_iY_i} = \frac{-\ddot{T}_i(t)}{T_i(t)} = \lambda^2 \tag{13}$$

$$D_iY_i'''' + pY_i'' - \lambda^2 m_iY_i = 0. \tag{14}$$

Assuming the mode shape to be the form $Y_i = e^{s_ix}$, substituting it into the above differential eqn (14), we obtain

$$D_is_i^4 + p_is_i^2 - m_i\lambda^2 = 0 \tag{15}$$

$$s_i = \pm\sqrt{\frac{-p_i + \sqrt{p_i^2 + 4D_i\lambda^2 m_i}}{2D_i}}, \quad \pm\sqrt{\frac{p_i + \sqrt{p_i^2 + 4D_i\lambda^2 m_i}}{2D_i}}\,i \tag{16}$$

(i.e. $s_i = \pm s_{1i}, \pm s_{2i}$).

Hence, the mode shape is a superposition of the above solutions associated with the exponential terms and can be expressed in the form

$$Y_i(x) = c_{1i}\cosh(s_{1i}x) + c_{2i}\sinh(s_{1i}x) + c_{3i}\cos(s_{2i}x) + c_{4i}\sin(s_{2i}x). \tag{17}$$

Substituting the mode shape $Y_i(x)$ into the boundary conditions, we can obtain a system of linear, homogeneous algebraic equations in the 16 variables c_{ij}, $i, j = 1, 2, 3, 4$ and the details can be expressed in the equations in the Appendix which are related to the length, the bending stiffness, the axial load, the mass per unit length of each region and the eigenvalue that is the natural frequency.

The 16 equations in the Appendix are homogeneous linear equations for 16 variables c_{ij}, $i, j = 1, 2, 3, 4$ and can be written in the following form

$$[N]\{C\} = \{0\}. \tag{18}$$

The characteristic frequency equation is satisfied for the existence of non-trivial solutions of the system. Therefore, the determinant of $[N]$ must be vanished, that is,

$$\text{Determinant } [N] = 0 \tag{19}$$

where $\{C\} = [c_{11}c_{21}c_{31}c_{41}c_{12}c_{22}c_{32}c_{42}c_{13}c_{23}c_{33}c_{43}c_{14}c_{24}c_{34}c_{44}]^{\mathrm{T}}$ the elements of $[N]$ are related to a, l_i, D_i, s_{1i} and s_{2i}.

From eqn (19), we can simultaneously get natural frequencies λ_j and mode shapes $Y_j(x)$ of the delaminated beam-plate. Once the free vibration problem is solved, the forced vibration analysis can be performed without difficulties.

4. FORCED VIBRATION ANALYSIS

We have investigated the free vibration of the delaminated beam-plate consisting of the natural frequencies and the mode shapes and now we focus on the forced vibration of the delaminated beam-plate. First of all, it is necessary to prove the existence of the orthogonality of $Y_j(x)$. The orthogonality of $Y_j(x)$ can be manifested as follows.

From eqn (14), we can obtain the following equation:

$$\lambda_j^2 m_i Y_{ij} = D_i Y_{ij}'''' + p_i Y_{ij}''. \tag{20}$$

Using eqn (20), integrating the product of the jth mode shape multiplied by the kth mode shape, the mass per unit length of ith segment and the square of the jth natural frequency or the kth natural frequency, we get the following two equations for each segment.

$$\lambda_j^2 \int_\alpha^\beta m_i Y_{ij} Y_{ik}\,\mathrm{d}x = (D_i Y_{ij}''' + p_i Y_{ij}')\,Y_{ik}|_\alpha^\beta - \left[\int_\alpha^\beta P_i Y_{ij}' Y_{ik}'\,\mathrm{d}x + D_i Y_{ij}'' Y_{ik}'|_\alpha^\beta - \int_\alpha^\beta D_i Y_{ij}'' Y_{ik}''\,\mathrm{d}x\right] \tag{21}$$

$$\lambda_k^2 \int_\alpha^\beta m_i Y_{ij} Y_{ik}\,\mathrm{d}x = (D_i Y_{ik}''' + p_i Y_{ik}')\,Y_{ij}|_\alpha^\beta - \left[\int_\alpha^\beta P_i Y_{ij}' Y_{ik}'\,\mathrm{d}x + D_i Y_{ik}'' Y_{ij}'|_\alpha^\beta - \int_\alpha^\beta D_i Y_{ij}'' Y_{ik}''\,\mathrm{d}x\right] \tag{22}$$

where α and β denote the starting and end point of each segment.

We can obtain the following eqn (23) by subtracting eqn (22) from eqn (21).

$$(\lambda_j^2 - \lambda_k^2) \int_\alpha^\beta m_i Y_{ij} Y_{ik}\,\mathrm{d}x = D_i(Y'''_{ij} Y_{ik} - Y'''_{ik} Y_{ij})|_\alpha^\beta + P_i(Y_{ij}' Y_{ik} - Y_{ik}' Y_{ij})|_\alpha^\beta - D_i(Y_{ij}'' Y_{ik}' - Y_{ik}'' Y_{ij}')|_\alpha^\beta. \tag{23}$$

Integrating the product of the jth mode shape multiplied by the kth mode shape from 0 to l, then we can obtain the following integral which contains four parts for the entire beam-plate.

$$(\lambda_j^2-\lambda_k^2)\int_0^l mY_jY_k\,dx=(\lambda_j^2-\lambda_k^2)\left[\int_0^{l_1} m_1Y_{1j}Y_{1k}\,dx+\int_0^{l_2} m_2Y_{2j}Y_{2k}\,dx\right.$$
$$\left.+\int_0^a m_3Y_{3j}Y_{3k}\,dx+\int_0^a m_4Y_{4j}Y_{4k}\,dx\right]. \quad (24)$$

Substituting eqn (23) into eqn (24), then the integral can be divided into three types which are the shear forces, the axial forces and the moments. Each type contains four parts. The complete integral can be written in the following by using the boundary conditions of eqns (10a)–(10d).

$$\begin{aligned}(\lambda_j^2-\lambda_k^2)&\int_0^l mY_jY_k\,dx\\
&=[V_{1k}(l_1)-V_{3k}(0)-V_{4k}(0)]Y_{1j}(l_1)-[V_{1j}(l_1)-V_{3j}(0)-V_{4j}(0)]Y_{1k}(l_1)\\
&\quad+[V_{2j}(0)-V_{3j}(a)-V_{4j}(a)]Y_{2k}(0)-[V_{2k}(0)-V_{3k}(a)-V_{4k}(a)]Y_{2j}(0)\\
&\quad+[M_{1j}(l_1)-M_{3j}(0)-M_{4j}(0)]Y'_{1k}(l_1)-[M_{1k}(l_1)-M_{3k}(0)-M_{4k}(0)]Y'_{1j}(l_1)\\
&\quad+[M_{2k}(0)-M_{3k}(a)-M_{4k}(a)]Y'_{2j}(0)-[M_{2j}(0)-M_{3j}(a)-M_{4j}(a)]Y'_{2k}(0)\\
&\quad+(p_1-p_3-p_4)Y'_{1j}(l_1)Y_{1k}(l_1)-(p_1-p_3-p_4)Y'_{1k}(l_1)Y_{1j}(l_1)\\
&\quad+(-p_2+p_3+p_4)Y'_{2j}(0)Y_{2k}(0)-(p_2-p_3-p_4)Y'_{2k}(0)Y_{2j}(0). \quad (25)\end{aligned}$$

Substituting the boundary conditions of eqns (10e)–(10p) into eqn (25), the integral will be vanished after some tedious algebra. Eventually, we come up with the following equation:

$$(\lambda_j^2-\lambda_k^2)\int_0^l mY_jY_k\,dx=0. \quad (26)$$

If j is not equal to k, it means that the square of jth frequency is not equal to the square of kth frequency, then we can assume that the integral of the product of the jth mode shape multiplied by the kth mode shape is vanished. Consequently, the orthogonality condition is established.

$$\int_0^l mY_jY_k\,dx=0 \quad \text{if } j\neq k. \quad (27)$$

To obtain the forced vibration response, we assume the displacement $u(x,t)$ as follows:

$$u_i(x,t)=\sum_{n=1}^{\infty} Y_{in}(x)T_n(t). \quad (28)$$

Substituting eqn (28) into eqns (8) and (9) and taking the advantages of the property of orthogonality, we should be able to derive the following equation after some algebra.

$$\ddot{T}_n(t)+\lambda_n^2T_n(t)=\frac{Q_n(t)}{\mu_n} \quad (29)$$

where the generalized force and the generalized mass can be written as follows:

$$Q_n(t) = \int_0^{l_1} (f(x,t) - 6p_1 a_1 x - 2p_1 b_1) Y_{1n}(x)\,dx + \int_0^{l_2} (f(x,t) - 6p_2 a_2 x - 2p_2 b_2) Y_{2n}(x)\,dx$$
$$+ \int_0^{a} (f(x,t) - 6p_3 a_3 x - 2p_3 b_3) Y_{3n}(x)\,dx + \int_0^{a} (-6p_4 a_4 x - 2p_4 b_4) Y_{4n}(x)\,dx \quad (30)$$

$$\mu_n = \int_0^{l_1} m_1 Y_{1n}(x)^2\,dx + \int_0^{l_2} m_2 Y_{2n}(x)^2\,dx + \int_0^{a} m_3 Y_{3n}(x)^2\,dx + \int_0^{a} m_4 Y_{4n}(x)^2\,dx. \quad (31)$$

From eqn (29) and the initial conditions which are the revised static initial deformation from eqns (11a)–(11d), we can achieve the solution of the generalized coordinates $T_n(t)$.

$$T_n(t) = T_n(0)\cos\lambda_n t + \frac{1}{\mu_n \lambda_n} \int_0^t Q_n(\tau)\sin\lambda_n (t-\tau)\,d\tau \quad (32)$$

where the initial generalized displacements can be expressed in the following form

$$T_n(0) = \frac{1}{\mu_n}\left[\int_0^{l_1} m_1 u_1(x,0) Y_{1n}(x)\,dx + \int_0^{l_2} m_2 u_2(x,0) Y_{2n}(x)\,dx\right.$$
$$\left. + \int_0^{a} m_3 u_3(x,0) Y_{3n}(x)\,dx + \int_0^{a} m_4 u_4(x,0) Y_{4n}(x)\,dx\right]. \quad (33)$$

Substituting eqn (32) into eqn (28), we can calculate the revised deformation and then substituting it into eqn (5), finally, we can obtain the forced vibration solution for the postbuckled delaminated beam-plate.

5. RESULTS AND DISCUSSIONS

The geometrical parameters in the one-dimensional model of the homogeneous strip delaminated beam-plate are the thickness ratio $\bar{h} = h_3/h$ and the length ratio $\bar{a} = a/l$. Furthermore, the axial compressive load p is normalized with respect to the critical axial load of a perfect beam-plate which is $4\pi^2 D_1/l^2$, that is $\bar{p} = p_1 l^2/4\pi^2 D_1$. Therefore, the postbuckling solutions to the delaminated beam-plate can be calculated by the combinations of the geometrical parameters and the axial load, as mentioned previously in Section 2. In our discussion, the material aluminum (Alloy 1100-H14, 99%Al) which consists of density 2710 kg m^{-3}, modulus of elasticity 70 Gpa and Poisson ratio 0.346 is chosen for the delaminated beam-plate. For convenience, we let the length of the 1st segment be 1/10 of the total length and assume the beam-plate is 2 m in length, 0.5 m in thickness, 1 m in width.

To study the postbuckling deformation, the deformation is nondimensionalized with respect to the thickness of the beam-plate, the horizontal position is normalized with respect to the length of the beam-plate. According to the figures of the postbuckling deformation, we can observe that the crack is completely open for some proper combinations of the geometrical parameters and the axial load. Besides, the deformation of the 3rd segment is obviously larger than the others, in other words, the deformation of the thinnest segment is largest. However, we can realize that the deformation becomes smaller as the decreasing

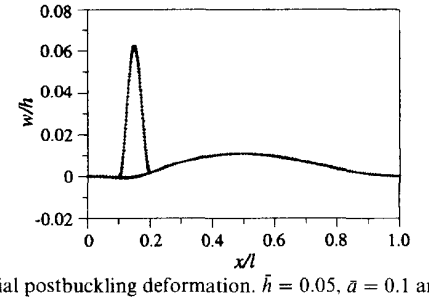

Fig. 2. Initial postbuckling deformation. $\bar{h} = 0.05$, $\bar{a} = 0.1$ and $\bar{p} = 0.6$.

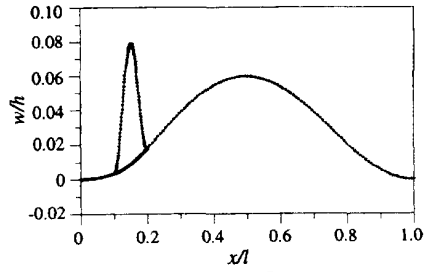

Fig. 3. Initial postbuckling deformation. $\bar{h} = 0.08$, $\bar{a} = 0.1$ and $\bar{p} = 0.9$.

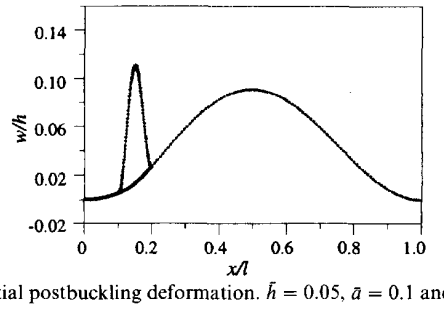

Fig. 4. Initial postbuckling deformation. $\bar{h} = 0.05$, $\bar{a} = 0.1$ and $\bar{p} = 0.9$.

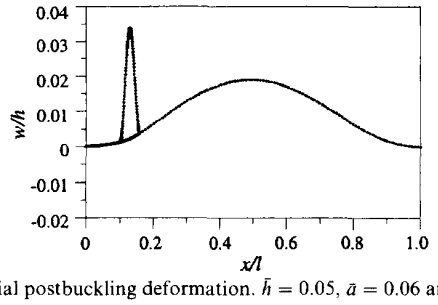

Fig. 5. Initial postbuckling deformation. $\bar{h} = 0.05$, $\bar{a} = 0.06$ and $\bar{p} = 0.9$.

axial load (see Figs 2 and 4 for two levels of the axial load $\bar{p} = 0.9$ and $\bar{p} = 0.6$), the decreasing length ratio (see Figs 4 and 5 for two levels of the length ratio, $\bar{a} = 0.1$ and $\bar{a} = 0.06$) or the increasing thickness ratio (see Figs 3 and 4 for two levels of thickness ratio, $\bar{h} = 0.08$ and $\bar{h} = 0.05$) are provided.

From eqn (20), we can obtain the mode shapes and the natural frequencies that are the roots of the characteristic equation by numerical method. For simplicity, only the first three mode shapes are plotted here. We may predict that if either the thickness ratio or the length ratio of the delaminated beam-plate is small, then the existence of the delamination does not significantly reduce the overall stiffness of the beam-plate. Thus, these mode shapes and frequencies are similar to the corresponding mode shapes and frequencies of the beam-plate under the same axial load. For the combination of $\bar{h} = 0.05$ and $\bar{a} = 0.06$, the mode shapes and frequencies are very much closer to the mode shapes and frequencies of the

Table 1. $\bar{h} = 0.05$, $\bar{a} = 0.1$ and $\bar{p} = 0.6$

	First five frequencies (rad s^{-1})
λ_1	2761.706543
λ_2	10162.421875
λ_3	21560.441406
λ_4	36742.968750
λ_5	55862.671875

Table 2. $\bar{h} = 0.08$, $\bar{a} = 0.1$ and $\bar{p} = 0.9$

	First five frequencies (rad s^{-1})
λ_1	1302.416992
λ_2	9051.052734
λ_3	20442.699219
λ_4	35515.648438
λ_5	54567.367188

Table 3. $\bar{h} = 0.05$, $\bar{a} = 0.1$ and $\bar{p} = 0.9$

	First five frequencies (rad s^{-1})
λ_1	1331.997314
λ_2	9059.617188
λ_3	20490.929688
λ_4	35661.468750
λ_5	54771.453125

Table 4. $\bar{h} = 0.05$, $\bar{a} = 0.06$ and $\bar{p} = 0.9$

	First five frequencies (rad s^{-1})
λ_1	1357.391602
λ_2	9066.953125
λ_3	20576.683594
λ_4	35829.109375
λ_5	54921.976562

perfect beam-plate. As the length ratio decreases from 0.1 to 0.06 the frequencies increase (see Tables 3 and 4 for two levels of the length ratio, 0.1 and 0.06) and as the thickness ratio decreases from 0.08 to 0.05, the frequencies also increase (see Tables 2 and 3 for two levels of the thickness ratio, 0.05 and 0.08). From the two phenomena, we realize that the stiffer delaminated beam-plate has the higher frequencies. As the compressive axial load decreases from 0.9 to 0.6, the first natural frequency increases so drastically that the first natural frequency under $\bar{p} = 0.6$ is the double of the first natural frequency under $\bar{p} = 0.9$ (see Tables 1 and 3 for two levels of the axial load, 0.6 and 0.9).

It should be noted that the sharpest part of the mode shape is the one of the 3rd segment and the amplitude is normalized with respect to the maximum amplitude of the mode shape. In the following discussion, we are only interested in the behavior of the fundamental model shape, since it is the most significant and dominant one among all the modes. First of all, the first mode shapes for two levels of axial load $\bar{p} = 0.6$ and $\bar{p} = 0.9$ indicate that the 3rd segment has a larger amplitude as the beam-plate has suffered a bigger

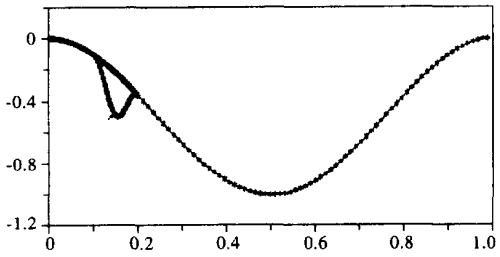

Fig. 6. First mode shape. $\bar{h} = 0.05$, $\bar{a} = 0.1$ and $\bar{p} = 0.6$.

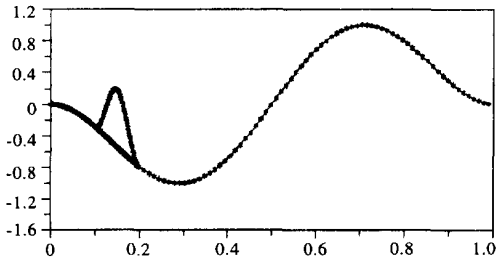

Fig. 7. Second mode shape, $\bar{h} = 0.05$, $\bar{a} = 0.1$ and $\bar{p} = 0.6$.

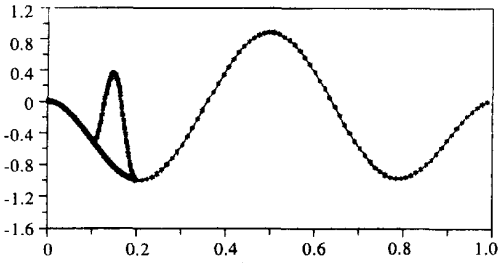

Fig. 8. Third mode shape. $\bar{h} = 0.05$, $\bar{a} = 0.1$ and $\bar{p} = 0.6$.

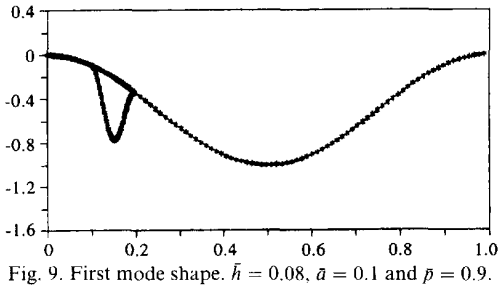

Fig. 9. First mode shape. $\bar{h} = 0.08$, $\bar{a} = 0.1$ and $\bar{p} = 0.9$.

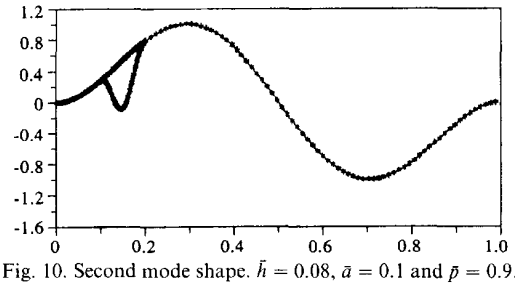

Fig. 10. Second mode shape. $\bar{h} = 0.08$, $\bar{a} = 0.1$ and $\bar{p} = 0.9$.

axial load (see Figs 6 and 12). Then, the mode shapes for two levels of thickness ratio, $\bar{h} = 0.05$ and $\bar{h} = 0.08$ show that the 3rd segment has a larger amplitude as the increasing thickness ratio is provided (see Figs 9 and 12). Finally, we notice the significant change of

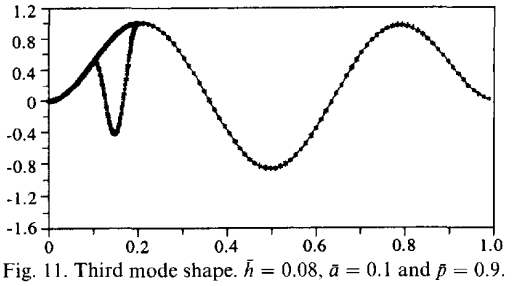

Fig. 11. Third mode shape. $\bar{h} = 0.08$, $\bar{a} = 0.1$ and $\bar{p} = 0.9$.

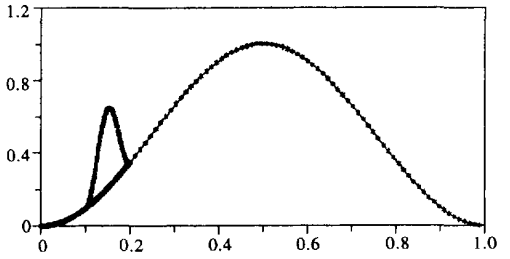

Fig. 12. $\bar{h} = 0.05$, $\bar{a} = 0.1$ and $\bar{p} = 0.9$.

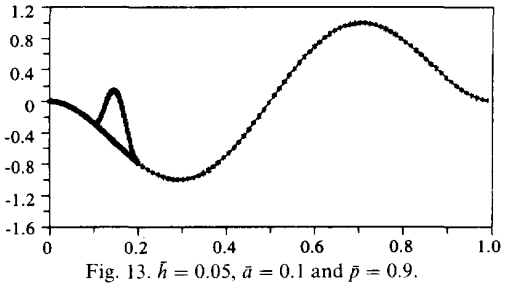

Fig. 13. $\bar{h} = 0.05$, $\bar{a} = 0.1$ and $\bar{p} = 0.9$.

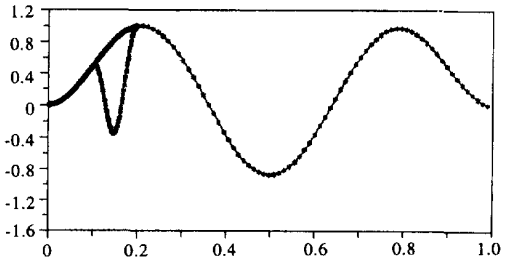

Fig. 14. $\bar{h} = 0.05$, $\bar{a} = 0.1$ and $\bar{p} = 0.9$.

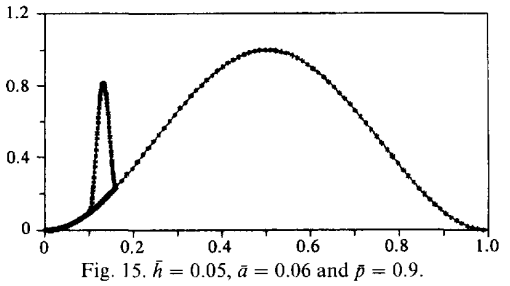

Fig. 15. $\bar{h} = 0.05$, $\bar{a} = 0.06$ and $\bar{p} = 0.9$.

the 3rd segment for the length ratio $\bar{a} = 0.06$ (see Fig. 15), that is, the sharpest mode shape appears as the length ratio is $\bar{a} = 0.06$. Hence, we presume that the mode shape of the 3rd segment is sensitive to the length ratio.

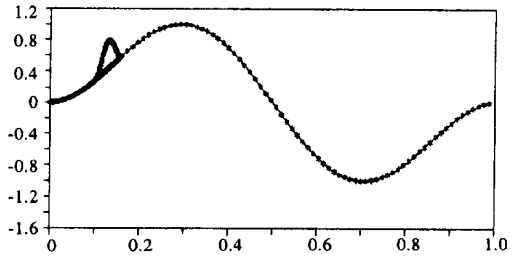

Fig. 16. $\bar{h} = 0.05$, $\bar{a} = 0.06$ and $\bar{p} = 0.9$.

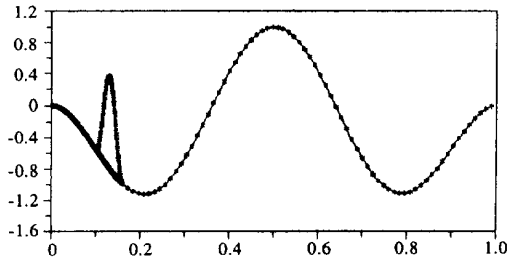

Fig. 17. $\bar{h} = 0.05$, $\bar{a} = 0.06$ and $\bar{p} = 0.9$

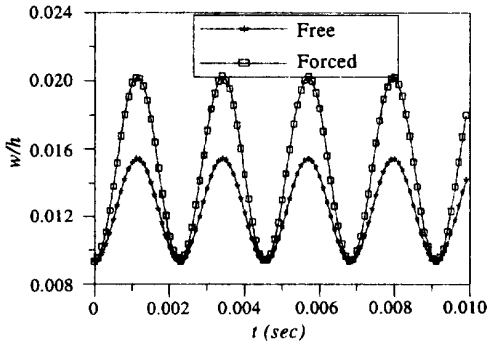

Fig. 18. Free and forced vibration responses under the constant force 10^4 kN. $\bar{h} = 0.05$, $\bar{a} = 0.1$ and $\bar{p} = 0.6$.

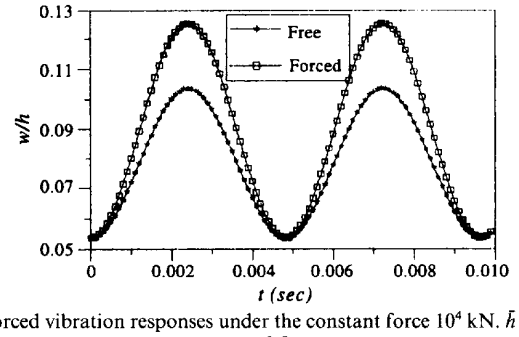

Fig. 19. Free and forced vibration responses under the constant force 10^4 kN. $\bar{h} = 0.08$, $\bar{a} = 0.1$ and $\bar{p} = 0.9$.

In forced vibration analysis, we study the vibration of the postbuckling delaminated beam-plate subjected to a constant uniform force, and the force must be huge enough to affect the amplitude of the deflection of the beam-plate, in other words, the amplitude of the deflection of the forced vibration will be visibly larger than that of the free vibration on the condition that the transverse applied load $f(x, t)$ is large enough. Because the axial load is greater than the critical axial load, we let the external constant force $f(x, t)$ be 1.0×10^4 kN. In order to search for the instant when the largest amplitude appears, the result of the deformation along with time is calculated at the middle of the 2nd segment, each one of

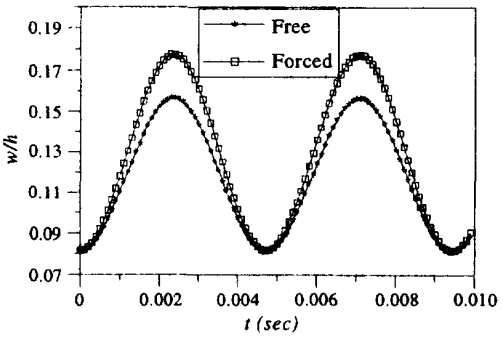

Fig. 20. Free and forced vibration responses under the constant force 10^4 kN. $\bar{h} = 0.05$, $\bar{a} = 0.1$ and $\bar{p} = 0.9$.

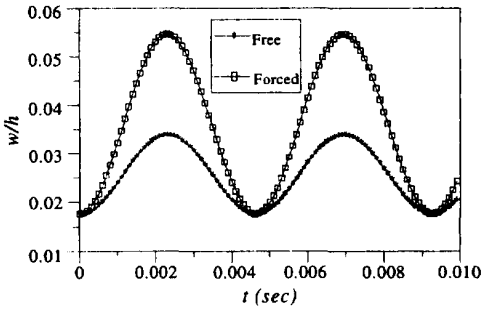

Fig. 21. Free and forced vibration responses under the constant force 10^4 kN. $\bar{h} = 0.05$, $\bar{a} = 0.06$ and $\bar{p} = 0.9$

the Figs 18–21 consist of the response of the free vibration and the forced vibration. The smaller amplitude is produced as the smaller axial load or smaller length ratio is applied (see Figs 18 and 21). Besides, it is worth noting that the period of Fig. 18 is almost half of the others, the reason is that the first frequency of Table 1 is double that of the others. The corresponding forced vibrations along with the position are shown from Figs 22 to 25 at the instant when the maximum deflection has occurred.

Finally, in order to complete the parametric study, the fundamental natural frequencies of the delaminated beam-plate are investigated for different delamination location, delamination size and delamination depth. It should be noted that the investigation is performed on the condition that only one parameter is varied and the other two parameters are fixed. As it can be seen from Fig. 26, the fundamental natural frequency is varied as the delamination location (namely, l_1/l) changes, besides, the symmetry of the result is observed and the fundamental natural frequency is smallest when the delamination location is at the middle of the beam-plate, which is quite reasonable. In Fig. 27, the fundamental natural

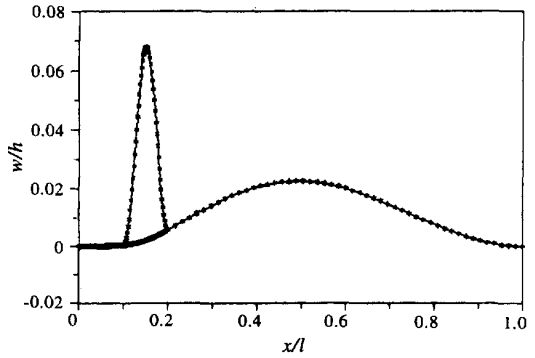

Fig. 22. Free and forced vibration responses under the constant force 10^4 kN. $\bar{h} = 0.05$, $\bar{a} = 0.1$ and $\bar{p} = 0.6$.

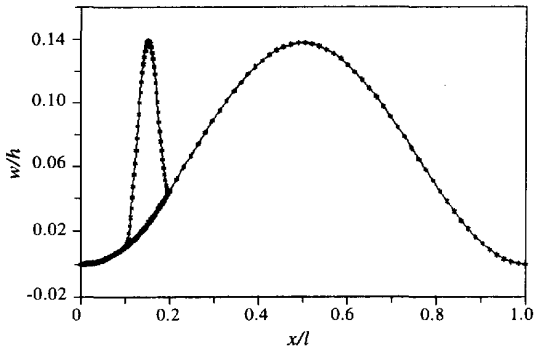

Fig. 23. Free and forced vibration responses under the constant force 10^4 kN. $\bar{h} = 0.08$, $\bar{a} = 0.1$ and $\bar{p} = 0.9$.

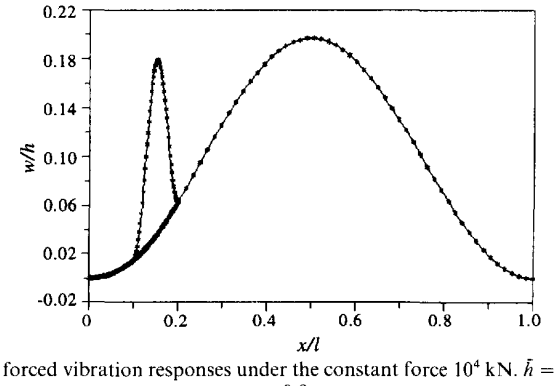

Fig. 24. Free and forced vibration responses under the constant force 10^4 kN. $\bar{h} = 0.05$, $\bar{a} = 0.1$ and $\bar{p} = 0.9$.

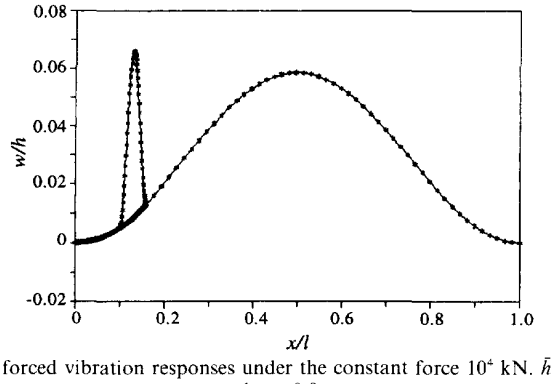

Fig. 25. Free and forced vibration responses under the constant force 10^4 kN. $\bar{h} = 0.05$, $\bar{a} = 0.06$ and $\bar{p} = 0.9$.

frequency is plotted for different delamination depth (namely, $\bar{h}$). It is noted that the minimum of the fundamental natural frequency occurs when the delamination depth is exactly half of the beam depth, which is also quite reasonable. In Fig. 28, the fundamental natural frequency is presented for a different delamination size (namely, $\bar{a}$). As can be seen, the fundamental natural frequency gets smaller as the delamination size gets larger, which is quite reasonable as well.

6. CONCLUSIONS

The vibrations of the delaminated beam-plate with respect to a static postbuckling state have been studied under the 1-D delamination model. If a beam-plate is under a

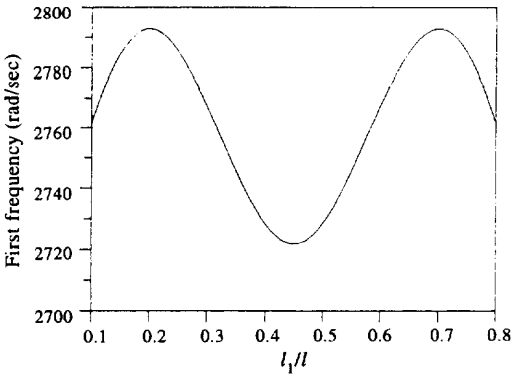

Fig. 26. Fundamental natural frequency for different delamination location (l_1/l).

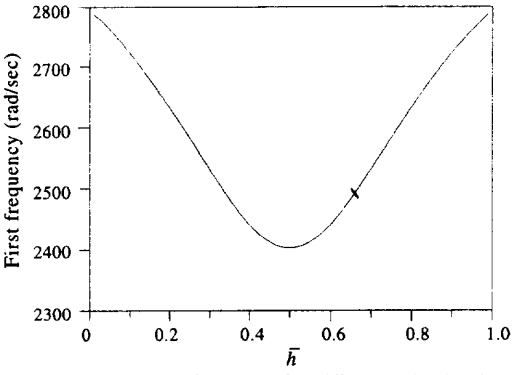

Fig. 27. Fundamental natural frequency for different delamination depth $\bar{h}$.

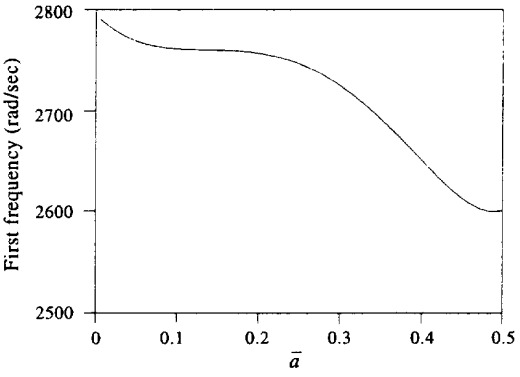

Fig. 28. Fundamental natural frequency for different delamination size $\bar{a}$.

postbuckled state, the natural frequencies and mode shapes of the structure will be substantially affected by the changes of the size and location of the delamination and by the magnitude of the axial compression. Based on the revised boundary conditions and governing partial differential equations, the free and forced vibrations of the beam-plate have been performed by separation of variables. We can predict the behavior of the postbuckling delaminated beam-plate subjected to an arbitrary distributed transverse force along with time and can avoid the collapse transverse force. In fact, only the across-the-width delaminations are considered in the present study. It may be worthwhile building a plate model, namely, two-dimensional (2-D) model for a general delamination. Furthermore it may be interesting to determine the location and size of the delamination of the beam by using the natural frequencies, mode shapes and the forced vibration responses of the beam.

Acknowledgement—This work was partially supported by the National Science Council of the Republic of China under Grant NSC 85-2212-E05-016. The authors are grateful for this support.

REFERENCES

Chen, H. P. (1991) Shear deformation theory for compressive delamination buckling and growth. *AIAA* **29,** 813–819.

Davila, C. G. and Johnson, E. R. (1993) Analysis of delamination initiation in postbuckled dropped-ply laminates. *AIAA* **31,** 721–727.

Jane, K. C. and Chen, J. C. (1995) Postbuckling deformation and vibration of a delaminated beam-plate with arbitrary delamination location. The master thesis of N.C.H.U. in Republic of China.

Kardomateas, G. A. and Schmueser, D. W. (1988) Buckling and postbuckling of delaminated composites under compressive loads including transverse shear effect. *AIAA* **26,** 337–343.

Kardomateas, G. A. (1989) Large deformation effects in the postbuckling behavior of composites with thin delamination. *AIAA* **27,** 624–631.

Meirovitch, L. (1967) *Analytical Methods in Vibrations*. MacMillan, New York.

Simitses, G. J., Sallam, S. N. and Yin, W. L. (1985) Effect of delamination of axially loaded homogeneous laminated plates. *AIAA* **23,** 1437–1444.

Shen, M. H. H. and Grady, J. E. (1992) Free vibrations of delamination beams. *AIAA* **30,** 1361–1370.

Wang, J. T. S., Liu, Y. Y. and Gibby, J. A. (1982) Vibration of split beams. *Journal of Sound and Vibration* **84,** 491–502.

Yin, W. L., Sallam, S. N. and Simitses, G. J. (1986) Ultimate axial load capacity of a delaminated beam-plate. *AIAA* **24,** 123–128.

Yin, W. L. and Fei, Z. (1988) Delamination buckling and growth in a clamped circular plate. *AIAA* **26,** 438–445.

Yin, W. L. and Jane, K. C. (1992) Vibration of a delaminated beam-plate relative to buckled states. *Journal of Sound and Vibration* **156,** 125–140.

APPENDIX

The above 16 equations are derived by substituting eqn (17) into the eqns (10a)–(10p) individually. In other words, eqn (A1) is derived from eqn (10a) and eqn (A2) is derived from eqn (10b) etc.

$$c_{11}+c_{31}=0 \tag{A1}$$

$$c_{21}s_{11}+c_{41}s_{21}=0 \tag{A2}$$

$$c_{12}\cosh(s_{12}l_2)+c_{22}\sinh(s_{12}l_2)+c_{32}\cos(s_{22}l_2)+c_{42}\sin(s_{22}l_2)=0 \tag{A3}$$

$$c_{12}s_{12}\sinh(s_{12}l_2)+c_{22}s_{12}\cosh(s_{12}l_2)-c_{32}s_{22}\sin(s_{22}l_2)+c_{42}s_{22}\cos(s_{22}l_2)=0 \tag{A4}$$

$$c_{11}\cosh(s_{11}l_1)+c_{21}\sinh(s_{11}l_1)+c_{31}\cos(s_{21}l_1)+c_{41}\sin(s_{21}l_1)=c_{13}+c_{33} \tag{A5}$$

$$c_{13}+c_{33}=c_{14}+c_{34} \tag{A6}$$

$$c_{13}\cosh(s_{13}a)+c_{23}\sinh(s_{13}a)+c_{33}\cos(s_{23}a)+c_{43}\sin(s_{23}a) = c_{14}\cosh(s_{14}a)+c_{24}\sinh(s_{14}a)+c_{34}\cos(s_{24}a)+c_{44}\sin(s_{24}a) \tag{A7}$$

$$c_{12}+c_{32}=c_{13}\cosh(s_{13}a)+c_{23}\sinh(s_{13}a)+c_{33}\cos(s_{23}a)+c_{43}\sin(s_{23}a) \tag{A8}$$

$$c_{11}s_{11}\sinh(s_{11}l_1)+c_{21}s_{11}\cosh(s_{11}l_1)-c_{31}s_{21}\sin(s_{21}l_1)+c_{41}s_{21}\cos(s_{21}l_1)=c_{23}s_{13}+c_{43}s_{23} \tag{A9}$$

$$c_{23}s_{13}+c_{43}s_{23}=c_{24}s_{14}+c_{44}s_{24} \tag{A10}$$

$$c_{13}s_{13}\sinh(s_{13}a)+c_{23}s_{13}\cosh(s_{13}a)-c_{33}s_{23}\sin(s_{23}a)+c_{43}s_{23}\cos(s_{23}a) = c_{14}s_{14}\sinh(s_{14}a)+c_{24}s_{14}\cosh(s_{14}a)-c_{34}s_{24}\sin(s_{24}a)+c_{44}s_{24}\cos(s_{24}a) \tag{A11}$$

$$c_{22}s_{12}+c_{42}s_{22}=c_{13}s_{13}\sinh(s_{13}a)+c_{23}s_{13}\cosh(s_{13}a)-c_{33}s_{23}\sin(s_{23}a)+c_{43}s_{23}\cos(s_{23}a) \tag{A12}$$

$$-D_1[c_{11}s_{11}^2\cosh(s_{11}l_1)+c_{21}s_{11}^2\sinh(s_{11}l_1)-c_{31}s_{21}^2\cos(s_{21}l_1)-c_{41}s_{21}^2\sin(s_{21}l_1)] + D_3[c_{13}s_{13}^2-c_{33}s_{23}^2]+D_4[c_{14}s_{14}^2-c_{34}s_{24}^2]=0 \tag{A13}$$

$$-D_2[c_{12}s_{12}^2 - c_{32}s_{22}^2] + D_3[c_{13}s_{13}^2\cosh(s_{13}a) + c_{23}s_{13}^2\sin(s_{13}a) - c_{33}s_{23}^2\cos(s_{23}a)$$
$$- c_{43}s_{23}^2\sin(s_{23}a)] + D_4[c_{14}s_{14}^2\cosh(s_{14}a) + c_{24}s_{14}^2\sinh(s_{14}a) - c_{34}s_{24}^2\cos(s_{24}a) - c_{44}s_{24}^2\sin(s_{24}a)] = 0 \quad \text{(A14)}$$

$$-D_1[c_{11}s_{11}^3\sinh(s_{11}l_1) + c_{21}s_{11}^3\cosh(s_{11}l_1) + c_{31}s_{21}^3\sin(s_{21}l_1) - c_{41}s_{21}^3\cos(s_{21}l_1)] + D_3[c_{23}s_{13}^3$$
$$- c_{43}s_{23}^3] + D_4[c_{24}s_{14}^3 - c_{44}s_{24}^3] = 0 \quad \text{(A15)}$$

$$D_2[c_{22}s_{12}^3 - c_{42}s_{22}^3] - D_3[c_{13}s_{13}^3\cosh(s_{13}a) + c_{23}s_{13}^3\sinh(s_{13}a) + c_{33}s_{23}^3\sin(s_{23}a)$$
$$- c_{43}s_{23}^3\cos(s_{23}a)] - D_4[c_{14}s_{14}^3\cosh(s_{14}a) + c_{24}s_{14}^3\sinh(s_{14}a) + c_{34}s_{24}^3\sin(s_{24}a) - c_{44}s_{24}^3\cos(s_{24}a)] = 0.$$